International Journal of Psychophysiology 97 (2015) 99–107

Contents lists available at ScienceDirect

International Journal of Psychophysiology

journal homepage: www.elsevier.com/locate/ijpsycho

# Looking for a precursor of spontaneous Sleep Slow Oscillations in human sleep: The role of the sigma activity

Danilo Menicucci [a,1], Andrea Piarulli [b,1], Paolo Allegrini [c], Remo Bedini [c,d], Massimo Bergamasco [b], Marco Laurino [c], Laura Sebastiani [a], Angelo Gemignani [c,d,e,*]

[a] Department of Translational Research on New Technologies in Medicine and Surgery, University of Pisa, via Savi 10, 56126, Pisa, Italy
[b] Perceptual Robotics Laboratory, Scuola Superiore Sant'Anna, Pisa, via Alamanni 13b, 56010, Pisa, Italy
[c] EXTREME Centre, Institute of Life Sciences, Scuola Superiore Sant'Anna, Piazza Martiri della Libertà 33, 56127, Pisa, Italy
[d] Institute of Clinical Physiology, National Research Council (CNR), via Moruzzi 1, 56124, Pisa, Italy
[e] Department of Surgical, Medical, Molecular and Critical Area Pathology, University of Pisa, via Savi 10, 56126, Pisa, Italy

ARTICLE INFO

*Article history:*
Received 27 January 2015
Received in revised form 12 May 2015
Accepted 13 May 2015
Available online 21 May 2015

*Keywords:*
Bistability
NREM sleep
Sleep slow oscillation
Spindle
Sigma band

ABSTRACT

Sleep Slow Oscillations (SSOs), paradigmatic EEG markers of cortical bistability (alternation between cellular downstates and upstates), and sleep spindles, paradigmatic EEG markers of thalamic rhythm, are two hallmarks of sleeping brain. Selective thalamic lesions are reportedly associated to reductions of spindle activity and its spectrum ~14 Hz (sigma), and to alterations of SSO features. This apparent, parallel behavior suggests that thalamo-cortical entrainment favors cortical bistability. Here we investigate temporally-causal associations between thalamic sigma activity and shape, topology, and dynamics of SSOs. We recorded sleep EEG and studied whether spatio-temporal variability of SSO amplitude, negative slope (synchronization in downstate falling) and detection rate are driven by cortical-sigma-activity expression (12–18 Hz), in 3 consecutive 1 s-EEG-epochs preceding each SSO event (Baselines). We analyzed: (i) spatial variability, comparing maps of baseline sigma power and of SSO features, averaged over the first sleep cycle; (ii) event-by-event shape variability, computing for each electrode correlations between baseline sigma power and amplitude/slope of related SSOs; (iii) event-by-event spreading variability, comparing baseline sigma power in electrodes showing an SSO event with the homologous ones, spared by the event. The scalp distribution of baseline sigma power mirrored those of SSO amplitude and slope; event-by-event variability in baseline sigma power was associated with that in SSO amplitude in fronto-central areas; within each SSO event, electrodes involved in cortical bistability presented higher baseline sigma activity than those free of SSO. In conclusion, spatio-temporal variability of thalamocortical entrainment, measured by background sigma activity, is a reliable estimate of the cortical proneness to bistability.


## 1. Introduction

Electrophysiological studies in animal models have revealed that during Slow Wave Sleep cortical neurons exhibit slow membrane-potential dynamical oscillations. This neuronal behavior is characterized by the coordinated switching of the membrane potential between a state of hyperpolarization (down state) and a state of firing activity with a rate similar to that of wakefulness (up state) (Steriade et al., 1993a; Vyazovskiy et al., 2009). This behavior, called neural bistability, typically lasts slightly more than 1 s and, when it involves a large amount of neurons in a coordinate way, represents the fundamental network phenomenon underlying different slow EEG patterns of Slow Wave Sleep, such as the K-complexes and the Sleep Slow Oscillations (SSO) (Amzica and Steriade, 1998; Massimini et al., 2004; Menicucci et al., 2009). These waves consist of an early positive deflection followed by a sharp negative peak (related to the cellular down state) and by a shallow positive half wave (related to the cellular up state) (Massimini et al., 2004; Menicucci et al., 2013; Laurino et al., 2014). The early positive deflection, spectrally characterized by the concurrent presence of high frequency activities, acts as a wake-like excitation, whose hypothesized role is that of triggering the down state on large scale (Menicucci et al., 2013; Laurino et al., 2014).

The concept that an early excitation favors the transition into the down state has been corroborated both theoretically and experimentally. In general, a perturbation acting on a system with two metastable states can force the transition to the lowest-energy one and this holds true also for the sleeping neurons (Wilson et al., 2006; Frohlich et al., 2006). At a computational level, depolarization-activated $K^+$ channels have been used to model bistability in the thalamo-cortical system:

*Abbreviations:* SSO, Sleep Slow Oscillation; NREM sleep, Non-Rapid-Eyes-Movement sleep; FRD, False Discovery Ratio; d.f., degrees of freedom.

* Corresponding author at: Department of Surgery, Medical, Molecular and Critical Area Pathology, University of Pisa, via Paradisa 2, 56124, Pisa, Italy. Tel.: +39 050 315 2686; fax: +39 050 580018.
*E-mail address:* gemignan@dfb.unipi.it (A. Gemignani).

[1] These authors contributed equally to this work.

http://dx.doi.org/10.1016/j.ijpsycho.2015.05.006
0167-8760/

simulations showed that the amount of depolarization influences the intensity of the $K^+$ current that induces the down state (Hill and Tononi, 2005). This mechanism has then been experimentally validated in ferret slices (Sanchez-Vives et al., 2010) and indirectly observed in humans. Specifically, Laurino et al. (2014), in a multisensory evoked K-complex experiment, showed that the higher the amplitude of the evoked wake-like excitation (P200), the higher the probability of effectively evoking the down state (N550). In principle, cortical proneness to bistability must depend on (i) the number of activity-dependent $K^+$ channels and (ii) their opening synchronization (Compte et al., 2003; Vyazovskiy et al., 2009; Sanchez-Vives et al., 2010). At the EEG level, both for SSO and K-complex, these two information are respectively estimated by means of the amplitude of the negative peak and by the "slope 1", i.e. the velocity of reaching the negative peak (Riedner et al., 2007; Laurino et al., 2014). Fig. 1 provides an illustration of the two features for a typical isolated SSO.

Once the aforementioned measures are adopted, it follows that the cortical proneness to bistability in humans displays a spatial variability across cortical areas with an antero-posterior gradient (Massimini et al., 2004; Menicucci et al., 2009). This kind of variability, stemming from averages over a sleep cycle, does not take into account time-varying properties. In general, however, a temporal variability of the proneness may take place, due, in turn, to variability in neural activity. Indeed, each SSO traveling event has its own topology and amplitude (Massimini et al., 2004; Riedner et al., 2007; Menicucci et al., 2009).

These two sources of variability, spatial and temporal, may be respectively associated to differences in anatomical structures, possibly explaining the antero-posterior gradient, and in functional modulations of GABAergic and glutamatergic neurons in the cortex (Steriade, 2000; Shu et al., 2003; Sanchez-Vives et al., 2010; Piantoni et al., 2013a).

Cortical proneness to bistability is influenced by subcortical structures, among which thalamus, up to now, seems to play a crucial role. The recent review of Crunelli and Hughes (2010) describes the emergence of the SSO as the product of the interaction between three cardinal oscillators: the cortical synaptically-based oscillator and two thalamic oscillators, the thalamocortical cells and the reticular thalamic neurons. On this basis,

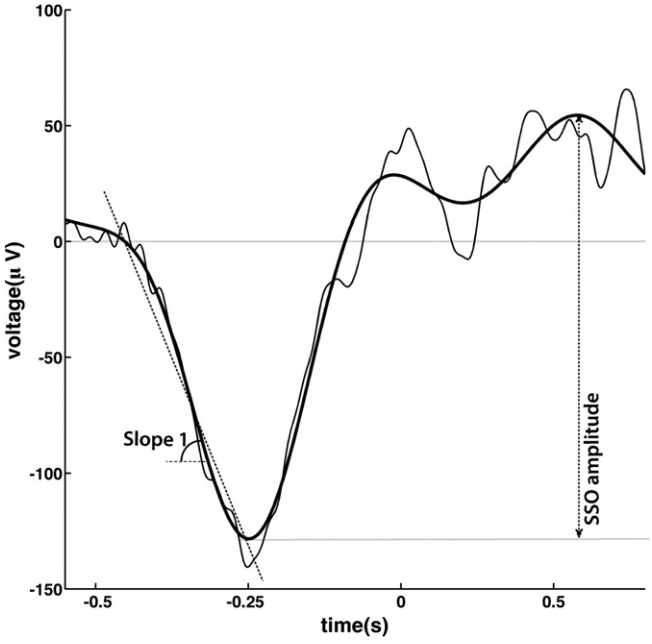


**Fig. 1.** Graphical definition of the SSO morphological features. The two superimposed lines represent the raw EEG trace of a SSO wave (thin line) and the corresponding delta-band filtered trace (thick line). Each detected wave is characterized by means of the SSO amplitude and the absolute value of the slope between the first zero crossing and the negative peak (slope 1) measured on the filtered signal according to the specifications in the Materials and methods section.

the detection on the cortex of SSO and its coalescing rhythms can only occur when the cortical and thalamic oscillators are entrained (Crunelli et al., 2015).

The contribution of the *thalamo-cortical entrainment* on the generation and synchronization of the cortical SSO has been highlighted or inferred by many studies in vitro (Rigas and Castro-Alamancos, 2007; Hirata and Castro-Alamancos, 2010; Wester and Contreras, 2013) and in vivo (Contreras et al., 1996a; Steriade, 2006; Gemignani et al., 2012; David et al., 2013; Menicucci et al., 2013; Piantoni et al., 2013b; Laurino et al., 2014).

As a recent confirmation of this viewpoint, a paradigmatic sign of thalamo-cortical activity, the sigma rhythm ~14 Hz (Contreras et al., 1996b, 1997; De Gennaro and Ferrara, 2003), was shown to characterize the spectrum of the positive deflection preceding spontaneous down states (Menicucci et al., 2013). More recently, Laurino et al. (2014), stimulating sensory cortices via afferent core thalamic projections, have confirmed the triggering of bistability (Laurino et al., 2014) only if the priming excitatory wave, along its travel towards integrative areas, undergoes a waxing mechanism, possibly thalamically driven. In addition, pathological models of thalamic degeneration and stroke highlight the fundamental role of the thalamo-cortical interaction for the SSO expression (Santamaria et al., 2000; Montagna et al., 2002; Gemignani et al., 2012).

The sigma rhythm observed at the cortical level corresponds to an intra-thalamic resonant activity in which thalamocortical cells are synchronized with the intrinsic oscillatory pattern of reticular thalamic neurons (Fuentealba and Steriade, 2005; Timofeev and Chauvette, 2011). This intra-thalamic activity becomes detectable on the EEG when the excitatory thalamocortical cells fire on their cortical targets (Fuentealba and Steriade, 2005; Timofeev and Chauvette, 2011). The cortex, however, does not play the role of a passive signal receiver but contributes to the within-thalamus synchronization via corticothalamic firing, which excites both reticular thalamic neurons and thalamocortical cells (Contreras et al., 1997; Timofeev and Chauvette, 2011; Bonjean et al., 2011). This cortico-thalamo-cortical entrainment has been reported to explain the occurrence of sigma-rhythm spindles upon the depolarizing phase of the SSO after the down state (Timofeev and Chauvette, 2011).

Notice that the described circuits have been recently proved to only sustain the so-called fast sigma activity (Doran, 2003). Indeed, a lower limit at ~12 Hz for the sigma activity related to *thalamo-cortical entrainment* has been better defined by recent studies on the differential properties of slow (centered around 10 Hz) and fast (centered around 14 Hz) sleep spindles. Indeed, the thalamo-cortical network seems involved only in the generation of fast spindles as they are selectively reduced after blocking low-threshold $Ca^{2+}$-dependent spike bursts in the reticular thalamic nucleus (Ayoub et al., 2013; Timofeev and Chauvette, 2013).

The aim of the present work is to describe whether the time-dependent proneness to bistability is marked by the presence of sigma rhythm, in other words, whether a pre-existing *thalamo-cortical entrainment* leads to an increase in the expression of SSOs in human EEG.

In order to provide evidence of this link we have studied temporally isolated SSOs and measured the sigma activity seconds before these SSOs (we call this temporal window "baseline").

In the following we report results showing baseline sigma activity as a reliable estimator of cortical proneness to bistability, able to predict SSO structure, mapping and dynamics.

## 2. Materials and methods

### 2.1. Subjects and sleep recordings

Ten non-sleep-deprived male volunteers (age 18–30, right-handed according to the Edinburgh Handedness Inventory, EHI) participated in the study. Inclusion criteria were: not taking any medication for at

least 1 year, no personal or family history of sleep disorders, and no medical, neurological or psychiatric disorders, as assessed by semi-structured interviews. In order to avoid variability related to the different phases of the menstrual cycle we chose to restrict our study to males since fast sigma activity has been shown to be influenced by reproductive hormones (Carrier et al., 2001). Note that these EEG recordings have been previously used in order to demonstrate the existence of a bump of wake-like excitation triggering the down state (Menicucci et al, 2013). The experimental procedures conformed with the World Medical Association Declaration of Helsinki and all participants signed an informed consent approved by the *Azienda Ospedaliero-Universitaria Pisana* Ethical Committee.

After an adaptation night, all volunteers were allowed to sleep at their usual bedtime and EEG recordings were carried out during the first sleep cycle of the night. During sleep, a 32-EEG channels monopolar amplifier (Nuamps, Neuroscan, Compumedics, El Paso, TX) was used to acquire signals with a sampling rate of 1 kHz and electrode impedance below 5 kΩ. During the recordings, scalp EEG signals were referenced to the FCz potential and then offline re-referenced to the average mastoids potential.

EEG epochs with artifacts were detected on the basis of an automated threshold-crossing detection algorithm (Piarulli et al., 2010) and verified by visual inspection. We discarded all those time segments containing artifacts in at least one channel. On average, 90% of recording time was free from artifacts. The artifact-free EEG segments were scored according to the AASM criteria (Iber et al., 2007) and analyzed using a previously published and validated SSO detection algorithm from our group (Menicucci et al., 2009; Piarulli et al., 2010).

### 2.2. Identification and analysis of temporally isolated SSO

SSOs were detected in the epochs belonging to N2 and N3 stages of the first sleep cycle using the Likeness Method proposed by our group in previous works (Menicucci et al., 2009; Piarulli et al., 2010). Herein we choose to focalize on the first sleep cycle because the SSO are homeostatically regulated and thus maximally expressed during the first sleep cycle (Riedner et al., 2007). Focusing on the first sleep cycle has also allowed to avoid any bias due to progressive electrode drying occurring from the second cycle on.

In summary, we classify as a SSO each wave consisting of (a) two zero crossings separated by 0.3–1.0 s, the first one having a negative slope; (b) a negative peak between the two zero crossings with a voltage less than −80 μV; (c) a negative-to-positive peak amplitude of at least 140 μV. Then, detected SSO events are completed by clustering full-fledged SSOs with concurrent similar waves, even if sub-threshold. These detection criteria naturally include all K-complexes (Massimini et al., 2004).

Moreover, in order to allow the assessment of unambiguous baseline epochs, specific of each SSO, without possible confounding effects of adjacent SSOs, we selected temporally isolated SSOs (Menicucci et al., 2013), herein defined as the events more distant than 7 s both from the previous and the following SSO event (time distances between events measured using negative peaks locations).

In the following, for the sake of simplicity we will refer to the temporally isolated spontaneous SSO using the acronym SSO.

### 2.3. Measures of cortical proneness to bistability

A straightforward *a posteriori* measure of the proneness is given by the detection rate of SSOs (Menicucci et al., 2009; Piarulli et al., 2010). Herein we use the average detection rate over the first sleep cycle. Other *a posteriori* estimates of proneness to bistability have the advantage of being computable event by event: These are the two morphological features of the SSO shown in Fig. 1 (see also Menicucci et al., 2009), namely the SSO amplitude and the slope of the EEG signal before the negative peak (slope 1). SSO amplitude is defined as the peak-to-peak voltage range and reflects how many pyramidal neurons synchronously undergo bistability (cellular down and up state); slope 1 is defined as the steepness of the wave between the first zero crossing and the negative peak and corresponds to the neuronal pool synchronization in falling into the down state (Esser et al., 2007; Vyazovskiy et al., 2007; Chauvette et al., 2010). These SSO parameters were measured on the signal filtered in the delta (0.5–4.0 Hz) band (for the filter implementation details see Menicucci et al., 2009 or Piarulli et al., 2010).

### 2.4. Measures of thalamo-cortical entrainment

We have adopted the EEG activity in the sigma band (12–18 Hz) as a measure of the *thalamo-cortical entrainment*. As earlier stated, we take 12 Hz as a lower boundary because of the demonstrated specificity of this band in involving thalamocortical circuits (Ayoub et al., 2013; Timofeev and Chauvette, 2013). The extension up to 18 Hz for the sigma band is in line with the works of Mölle et al. (2002) and of Menicucci et al. (2013): these works have demonstrated that despite sigma activity is centered around 12–15 Hz, its effect spreads over higher frequencies. As a beneficial side effect this choice also allows for a better time resolution.

We computed the time–frequency power spectrum (spectrogram) of all EEG epochs preceding an SSO event, starting from 4 s before the negative peak and ending 1 s before the peak itself. This ending point occurs before the early positive deflection (Menicucci et al., 2013) and thus the three-seconds epoch is appropriate for estimating the baseline activity before the SSO. The spectrogram has a time–frequency step of 66 ms and 6 Hz and is calculated by the Fast Fourier Transform applied on Hamming-weighted sliding-window on each three-seconds epoch. Each window has a time-width of 166 ms with a 60% overlap between contiguous windows.

In line with the approach of Menicucci et al. (2013), we split the three-seconds epoch in three one-second-baseline windows (B3, B2, B1, with B1 corresponding to the interval nearest to the negative peak). This was done to verify whether sigma activity either (i) acts as trigger for SSO (a specific association with a narrow time interval was expected in this case), or (ii) modulates SSO as an expression of a slow-varying background activity (a similar association for all the three 1 s baselines was expected, only slowly reinforcing when passing to the closer interval).

For each of the three baselines, sigma activity was measured by averaging the sigma band of the spectrogram in the corresponding 1 s window. All statistical analyses were replicated for B1, B2 and B3 and significance levels were then adjusted taking into account the multiple testing issue on the basis of False Discovery Ratio (FDR) approach (Benjamini and Yekutieli, 2001).

### 2.5. Measuring thalamic influence on cortical proneness to bistability

This section is devoted to describing how we investigated the association of baseline sigma activity with SSO features (amplitude, slope 1, rate and cortical spreading). In particular we investigated whether the baseline sigma activity showed: (A) average scalp maps that matched SSO features (spatial variability; Fig. 2A); (B) event-by-event power variability that paralleled the event-by-event SSO amplitude and slope 1 variability (event-by-event shape variability; Fig. 2B); and (C) an event-by-event topological power variability that affected SSO cortical spreading (event-by-event spreading variability; Fig. 2C). In all analyses, both SSO features and sigma power levels have been corrected for the *subject effect* by applying for each test an appropriate correction method. For the analysis of spatial variability, the subject effect was removed by subtracting from each data set (for each variable and each subject) its average value calculated over the scalp electrodes; this allowed to preserve the scalp variability and thus to use the corrected variables for sigma-SSO correlations.

For the study of the event-by-event association between baseline sigma activity and SSO expression (analysis of event-by-event shape

variability and analysis of event-by-event spreading variability), the subject effect was removed by subtracting from the event data series related to each electrode and subject, the average value calculated over the subject and the electrode; this correction removed also the different between-subjects fronto-posterior gradient and thus it allowed focusing solely on the event-by-event variability.

(A) *Analysis of spatial variability*

Maps of SSO amplitude, slope 1 and detection rate were compared to those of baseline sigma activity (measures in dB). Map similarities for the three SSO features with respect to sigma were measured by means of the Pearson correlation (threshold of significance $p < 0.01$) calculated on scatterplots, where each point corresponds to one of the 29 retained electrodes (Fig. 2A). All values in the scatterplots correspond to the average over all events belonging to N2 and N3 stages. The statistical significance of correlations was established by using as threshold $r_t = 0.45$ that is the highest coefficient obtained between the frequencies around the 50 Hz power line (45 Hz–55 Hz) and the SSO features (in line with Menicucci et al., 2013). This coefficient does not correspond to a real association because the power line is clearly independent from the brain activity; thus it can be considered an appropriate threshold to discriminate meaningful from fortuitous (by chance) correlations. This criterion was more stringent than the classical rule based on the Fisher z-transformation, even at p-value threshold <0.001.

Besides, possible spurious, i.e. non-functional correlations, possibly related to non-sleep networks and volume conduction, have been checked; in other words, since independent processes originating around the same brain area have a similar activity distribution over the cortex, results of spatial variability analysis may suffer from geometrical fixed factors that could falsely associate functional phenomena, which are actually independent. In order to amend this possible pitfall we used the upper alpha EEG power (10–12 Hz) (Klimesch, 1999) of the relaxed wake as a control condition for sleep sigma activity. Invariant correlations (i.e., independent of the sleep/wake state) would indicate false functional associations. The appropriateness of this control procedure stems from similarities of alpha and sigma rhythms in both frequency range and waxing and waning (spindle) behavior. Actually, both activities derive from the loop involving thalamic reticular, thalamocortical and pyramidal cortical neurons. For the sake of completeness, we recall that thalamo-cortical neurons with high-threshold $Ca^{2+}$ channels sustain alpha rhythm while thalamo-cortical neurons with low-threshold $Ca^{2+}$ channels sustain sigma activity (Hughes and Crunelli, 2005, 2007; Vijayan and Kopell, 2012).

EEG of relaxed wake epochs were derived from ten-minutes resting-state EEG recordings performed before sleep. The same EEG montage and referencing was used for wakefulness and sleep recordings and this allowed a precise electrode match between the two conditions. In order to record the relaxed wakefulness EEG epochs, subjects were asked to keep their eyes closed, to relax, to refrain from moving, and to avoid any structured mental activity. The wake-EEG was visually inspected and head-movement-corrupted epochs were discarded (a total of 10–20 s epochs present in 2 out of 10 subjects). Eye-movement artifacts were corrected by means of the application of the temporal-constrained ICA (James and Gibson, 2003).

(B) *Analysis of event-by-event shape variability*

This analysis, performed electrode by electrode, consisted in taking into account all SSO events in which the electrode was involved. For each electrode, we calculated the Pearson correlations between baseline sigma power and the morphological feature (be it amplitude, or slope 1) of the following SSO wave (Fig. 2B). According to the different number of SSO detected under each electrode (that ranged from 70 to 350 in our dataset), the Pearson correlations were calculated between series of variable length. The threshold for statistical significance was selected as $p < 0.01$ at the lower number of events that corresponds to $r = 0.31$.

(C) *Analysis of event-by-event spreading variability*

We verified whether the presence of a temporary increase of baseline sigma activity in a cortical region marked a preferential area of spreading for the following SSO. Here and in the following we will use the term “event spreading” to indicate

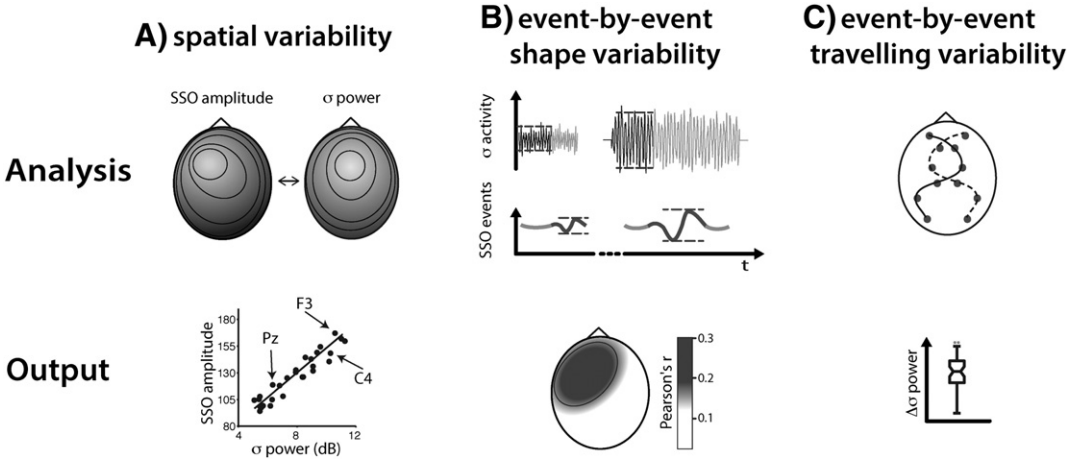


**Fig. 2.** Summary of the methods for studying the associations between baseline sigma (σ) activity and SSO expression. Panel A (first column). Spatial variability analysis. The analysis aims at associating the average scalp distributions of a SSO feature (SSO amplitude, in the pictorial example on the first row, left) and of the baseline sigma power (first row, right). The similarity between scalp maps is measured by means of Pearson correlation calculated between the series of sigma power and SSO features derived from each electrode and averaged over SSO events (second row). Panel B (second column). Event-by-event shape variability. The analysis aims at associating the event-by-event variability of baseline sigma activity with that of SSO shape. The first row shows two cases of baseline sigma activity (black epochs in the upper trace of the first row) with the following SSOs (lower trace of the first row) related to a representative electrode. Correlation between baseline sigma power and each morphological feature of the corresponding SSO is performed for each electrode by means of Pearson correlation performed over the events. The analysis yields a correlation map as shown on the second row. Panel C (third column). Event-by-event spreading variability. The first-row figure illustrates an example of the intra-event comparison analysis that considers a SSO event spreading on the solid path at time *t*. The method compares the baseline sigma activity along the solid path with the concurrent sigma activity over the homologous path, indicated by the dashed line, symmetrical with respect to the midline. Differences between sigma activities are evaluated by comparing the average powers over each pathway. The box plot of Δsigma power (Δσ) is shown in the second row.

the set of electrodes involved in a SSO event. This term intuitively denotes the variable and irregular composition of the set. As depicted in Fig. 2C, we compared the baseline sigma activity detected on the electrodes belonging to a SSO event to the activity of homologous electrodes spared by the same SSO event. Such an intra-event comparison avoids confounding effects caused by slowly varying biochemical processes such as those associated to sleep deepening. Moreover, this intra-event approach was specifically designed to avoid spatial confounding effects as it is based on comparison between homologous electrode pairs (symmetric electrodes with respect to midline, e.g. F3–F4, C3–C4, O1–O2).

In detail, we selected all SSO events whose propagation did not contain any homologous pair. We compared the baseline sigma activity over the event spreading (solid line in Fig. 2C) with the baseline sigma activity over the ensemble of the homologous electrodes (symmetrical dashed line in Fig. 2C), disregarding midline electrodes. For each pair of homologous electrodes we calculated the Normalized Difference of Power — NDP = $(p_e - p_h) / (p_e + p_h)$, where $p_e$ is the power of the electrode belonging to the event and $p_h$ that corresponding to its homologous — each event was characterized by the NDP averaged over the event spreading.

The normalization $1 / (p_e + p_h)$ was introduced in order to have similar contributions of the different electrodes to the average difference over the event spreading. A Wilcoxon signed rank test performed on all spreading events verified the null hypothesis that NDP data come from a distribution with zero median and indicated the statistical significance of the sigma power difference between events spreading and the ensemble of their homologous electrodes. The threshold for statistical significance was set at $p < 0.01$.

## 3. Results

Isolated SSOs were identified according to the selection criteria described in the Materials and methods section. Fig. 3 shows the raw EEG signals immediately before and during typical SSOs. It is worth noting that sigma activity, usually present as a spindle (like the activity in the examples) in the up state following the down state, is also present in the baseline epochs before the SSO.

### 3.1. Baseline sigma activity maps cortical proneness to bistability

Upon the analysis of spatial variability, the scalp maps of SSO detection rate, SSO amplitude and slope 1 resulted highly correlated ($p < 0.01$, d.f. = 28, FDR corrected) with the scalp map of baseline sigma activity power (Fig. 4). These correlations did not significantly change as a function of the different baseline windows (Table 1). As a control condition for the associations with the sleep sigma activity, we verified the correlations between the SSO features and the high alpha band power of the relaxed wakefulness. High alpha activity shows a more posterior distribution (Fig. 4) and correlations with SSO features that resulted weaker and below the threshold of statistical significance (scatterplots in Fig. 4 and Table 1).

### 3.2. Baseline sigma activity fluctuations shape SSO amplitudes

The analysis of *event-by-event shape variability* allowed us to identify some cortical areas showing a significant positive association between the variability in time of baseline sigma power and that of SSO amplitude. Fronto-central areas showed the highest correlations ($|r| > 0.3$ corresponding to a significance $p < 0.01$, d.f. = 69). The topological extension of the correlation increased moving from B3 to B1, namely approaching the onset of the SSO (Fig. 5). No significant correlations for slope 1 were found.

### 3.3. Baseline sigma activity stands out along the SSO cortical spreading

The analysis of event-by-event spreading variability was based on the subset of SSO events whose propagation did not contain any homologous pair (65 SSO events) and it showed that baseline sigma activity was significantly ($p < 0.01$, FDR corrected) higher for the electrodes belonging to event spreading compared to the homologous ones, spared by the event. This association was confirmed for each baseline interval (B1, B2, B3) (Fig. 6).

## 4. Discussion

This study shows that the occurrence of spatio-temporal patterns of sigma activity, preceding the onset of the SSO and reflecting time-dependent thalamo-cortical *entrainment*, is a reliable precursor of the dynamical establishment of the cortical proneness to bistability during NREM sleep in humans. In particular, variations in structure, mapping and dynamics of Sleep Slow Oscillations (SSOs) are accompanied by corresponding changes of the preceding sigma power, that are stable for seconds. We have demonstrated that baseline sigma power, detected in the background EEG activity preceding the SSO event by few seconds: (i) maps cortical proneness to bistability during NREM sleep; (ii) has temporal fluctuations that correlate with the amplitude of the corresponding SSO; (iii) stands out along the SSO cortical travel.

For point (i), the areas with higher (lower) sigma activity in the three baselines are those with higher (lower) SSO rate and amplitude, and steeper (shallower) slope 1. We stress that this result highlights that these associations are topological, as confirmed by the electrode-by-electrode scatter plots of the baseline sigma power versus SSO features, both averaged over the first sleep cycle (Fig. 4).

The lack of significant correlations between high-alpha activity recorded during wakefulness, which shares the same thalamo-cortical circuits generating sleep spindles, and SSO features rules out any trivial associations, due either to anatomical wirings or volume-conduction-based effects between sigma and SSOs.

This corroborates the growing evidence that the thalamus plays a key role in modulating the SSO (Steriade et al., 1993b; Contreras and Steriade, 1996; Crunelli and Hughes, 2010), although the SSO has been shown to survive also when the thalamus is absent (Timofeev et al., 2000; Compte et al., 2003; Sanchez-Vives et al., 2010). Selective thalamic degeneration models, such as the Fatal Familial Insomnia in humans, (see Montagna et al., 2003 for a review) confirm this association. In the Fatal Familial Insomnia, the lesion mainly involves the medial dorsal nucleus (connected with prefrontal and cingulate cortices) that is believed to play a crucial role in patterning thalamic activity of sleep spindles (Steriade and Deschenes, 1984; Marini et al., 1989). Indeed, our group has recently studied a FFI patient in the middle course of the disease and has found that the significant reduction of sigma activity in fronto-central regions (Gemignani et al., 2012; see supplementary Fig. 3 therein), i.e. the projection of the medio dorsal nucleus (Ward, 2011), occurs with a reduction of SSO rate and with the fading of spindles crowning the up state (Gemignani et al., 2012; Fig. 4 therein).

The results of point (ii) and (iii) indicate that this association holds true also along the temporal domain as depicted by event-by-event associations shown in Figs. 5 and 6. The correlation maps of event-by-event shape variability (point ii) indicate that, only in fronto-central areas, the recruitment of neural population synchronously involved in SSO behavior seems to be promoted by the amount of preceding sigma activity. Accordingly, the results regarding event-by-event spreading variability (point iii) indicate that SSOs *preferably* spreads within areas with the highest sigma activity in the baseline. The choice of homologous electrodes as a "control ensemble" is appropriate since the sigma activity detected by EEG is expression of the matrix thalamic

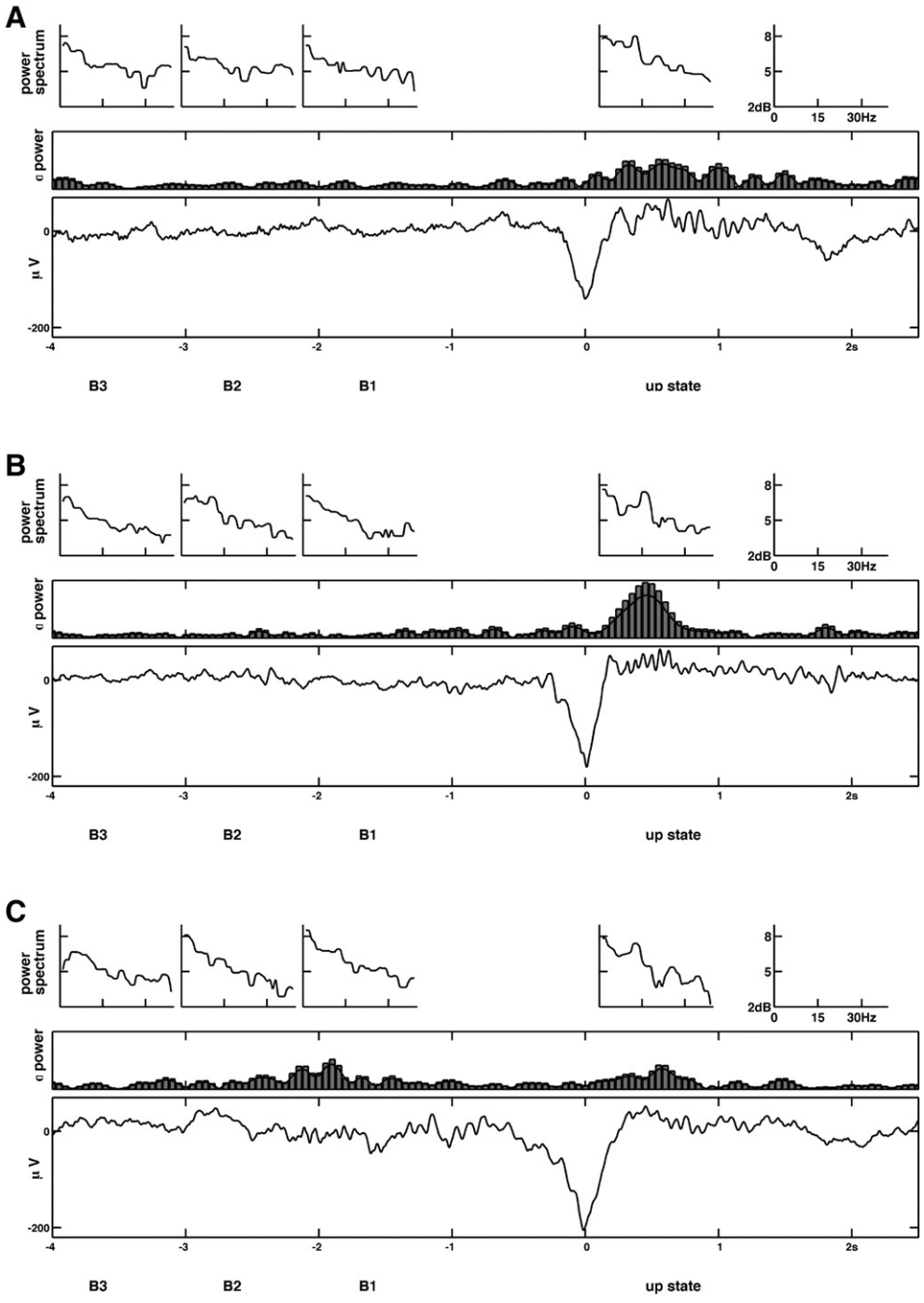


**Fig. 3.** Examples of the EEG traces with SSO. For each of the three example of EEG traces containing isolated and full-fledged SSOs (panels A, B, C), the lower row shows the raw signal from 4 s before the negative peak of the SSO to 2.5 s after it. The three 1 s' baseline windows are defined from minus 4 s to minus 1 s (B3, B2, B1); the up state is defined from 0.2 s to 1.2 s from the negative peak (centered on 0). The middle row shows the amplitude of sigma (σ) power in time, in the 12–18 Hz interval, estimated according with the specifications in the Materials and methods section. The four spectrograms in the upper row show the power spectrum distributions of the 3 baselines and of the upstate. Panel A shows a long-lasting spindle in the upstate preceded by not spindle-like sigma activity in the baselines. Panel B shows a full-fledged spindle in the upstate preceded by not spindle-like sigma activity in the baselines. Panel C shows a spindle-like sigma activity both in the upstate in the baselines. Only spectrograms of the up states clearly show a peak within the sigma band (~15 Hz).

system, which is diffuse, and does not show any lateralization (Dehghani et al., 2010; Bonjean et al., 2012). The aforementioned results lead us to conjecture that sigma-activity patterns emerge out of the background activity paving the way to the traveling of SSO.

What is the peculiarity of sigma activity preceding the down state? In humans some works have identified a bump of sigma activity preceding the down state (Menicucci et al., 2013; Piantoni et al., 2013b). As shown in healthy adults (Menicucci et al., 2013, Fig. 3) and in healthy children (Piantoni et al., 2013b, Fig. 1), the falling in down state is preceded by an increase of sigma and gamma activity. In the same framework Laurino et al. (2014) have recently demonstrated that the early positive deflection preceding an evoked down state can be considered as a wake-like traveling excitation. We infer that this early positive bump is able to trigger activity-dependent $K^+$ channels (Frohlich et al., 2006; Sanchez-Vives et al., 2010) in cortical areas with higher proneness to bistability via a thalamic interplay. In this light, baseline sigma activity could cluster excitatory activities facilitating cortical neurons to transit from a wake-like activity to down state; namely, the sigma

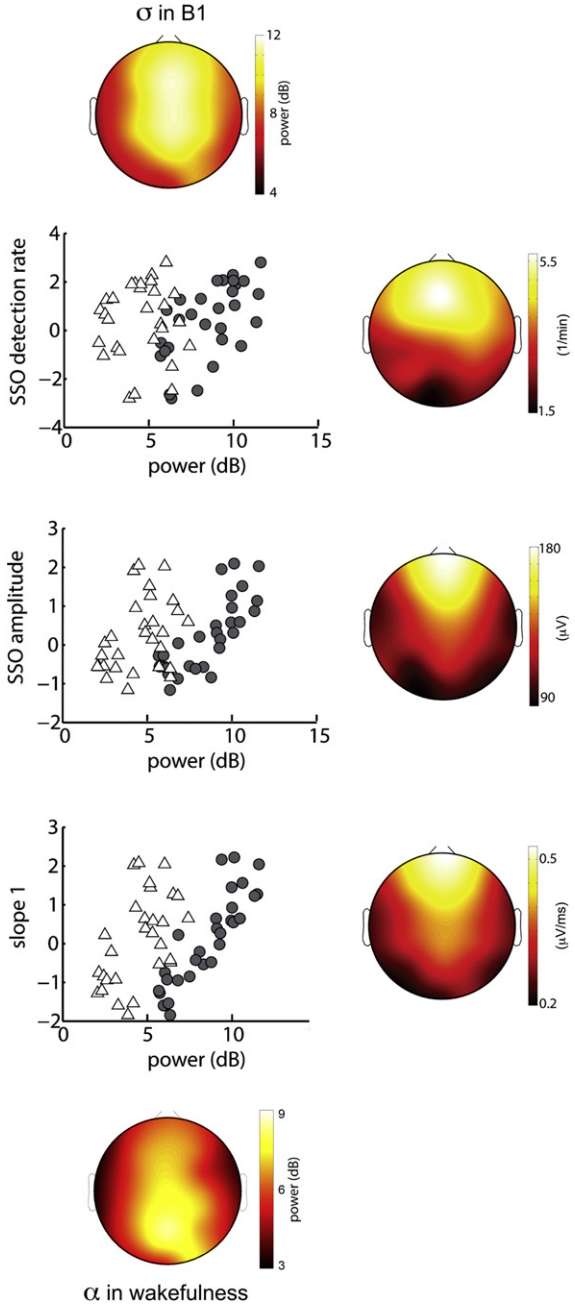


**Fig. 4.** Scalp distribution of sigma activity and of SSO features. On the top (first column, first row) the group-average topographic plots of sigma power during the B1 baseline, and on bottom (first column, fifth row) the topographic plot of the high alpha activity estimated during the relaxed wakefulness, recorded before sleep. Second, third and fourth rows contain two graphics each: the topographic plot of a feature of the isolated SSO events, on the right (second column) and, on the left (first column) the scatterplots of sigma power versus the corresponding SSO feature. The second row refers to the SSO detection rate, the third one to the SSO amplitude, and the fourth to slope 1. Solid circles show the significant correlation between the average level (over the events) of sigma power under an electrode and the corresponding average of each SSO parameter. Open triangles show the non-significant correlation between sigma power and high alpha activity (see text for details).

activity could favor the positive bump preceding the SSO downstate (Menicucci et al., 2013). The positive deflection preceding spontaneous down states seems to play the same role of P200 in evoked K-complexes (Laurino et al., 2014).

As a synthesis, the positive deflection with a bump of wake-like activity is favored by background oscillatory activity in sigma band.

**Table 1**
Correlations between baseline sigma activity and morphological features of the following SSO.

| | NP amplitude | Detections rate | Slope 1 |
|---|---|---|---|
| WAKE[a] | 0.2745 | 0.1004 | 0.4383 |
| B3 | 0.8402[b] | 0.7186[b] | 0.9005[b] |
| B2 | 0.8784[b] | 0.7645[b] | 0.9190[b] |
| B1 | 0.8738[b] | 0.8000[b] | 0.9292[b] |

[a] Correlations with high alpha power during relaxed wakefulness.
[b] Marks correlation values above the 50 Hz threshold.

This scenario can be thought as a process composed of two phases: a thalamic preparation phase visible in the baseline (sigma activity) and an emerging cortical phase (early positive bump).

The thalamic preparation phase is associated with excitatory inputs from thalamo-cortical cells onto dendrites of pyramidal neurons, opening the door to subsequent integrated cortical network activities (Sejnowski and Destexhe, 2000) in the form of the early positive bump. This happens with higher probability for those cortical circuits that have been synaptically upscaled during wakefulness (Feinberg and Campbell, 2010; Tononi and Cirelli, 2014). As a final outcome, the opening of $K^+$ channels (i.e. downstate), favored by gamma activity of the early positive bump, prevents any further integration (Allegrini et al., 2013).

The last result that sigma activity stands out along the SSO cortical travel, can thus be interpreted in the light of what we have said. In other words we were able, event by event, to topologically associate the excitatory phase to a preceding thalamic preparatory phase. We propose that the SSO spreading results from the complex and topological interplay between synaptically cortical upscaled circuits and thalamic sigma slow fluctuations. Still, the irregular and always changing spreading of SSO events remains to be understood and explained.

Its variability may be connected to the infraslow oscillations (0.02–0.2 Hz), whose phase has been shown to affect the spontaneous occurrence of both K-complexes and fast-rhythm bumps and that might represent the electrophysiological background scenario linking sigma and SSO (Vanhatalo et al., 2004, 2005). Infraslow oscillations as a latent factor contributing to the cortical proneness would be fast enough to modulate excitability between consecutive isolated SSOs, and at the same time slow enough to be invariant during the three baselines B1, B2 and B3. At present, the nature of infraslow oscillation remains elusive. Some studies indicate that they are a typical feature of the thalamus, since have been recorded in slices of thalamic relay nuclei, hypothetically related to some long-lasting and slow propagating hyperpolarizing potentials (see Hughes et al., 2011 for a review). We cannot exclude that slow changes of cortical excitability during sleep could be also driven by the activity of brainstem structures or nuclei such as the GABAergic parafacial zone (Anaclet et al., 2014) and some cholinergic nuclei (Steriade et al., 1993c; Steriade, 2004; Valencia et al., 2013).

It has been suggested that the periodicity of the time scales of infraslow oscillations, regardless of their origin, yields a peculiar EEG pattern called Cyclic Alternating Pattern (CAP) (Parrino et al., 2006). We have previously (Menicucci et al., 2013) described the isolated SSO as one of the atomic structures of A1 sub-types of CAP, that is the time domain in which arousal events are grouped during sleep with the same dynamics of infraslow oscillations (Parrino et al., 2006). The isolated SSO could represent a borderline case of CAP in which the duration of the A phase is limited to a single slow wave. In this view, the early excitation initiating spontaneous SSOs would correspond to a microarousal and the following downstate to an anti-arousal swing, both "weaved into the texture of sleep taking part in the regulation of the sleep process" (Halász et al., 2004; Ferri et al., 2006). The link between SSO and anticipatory thalamo-cortical entrainment suggests a physiological basis of the alternation between A (activation) and B (deactivation) phases of the CAP (Terzano and Parrino, 1993): increased cortical activity forced by the thalamic entrainment could favor the bistability.

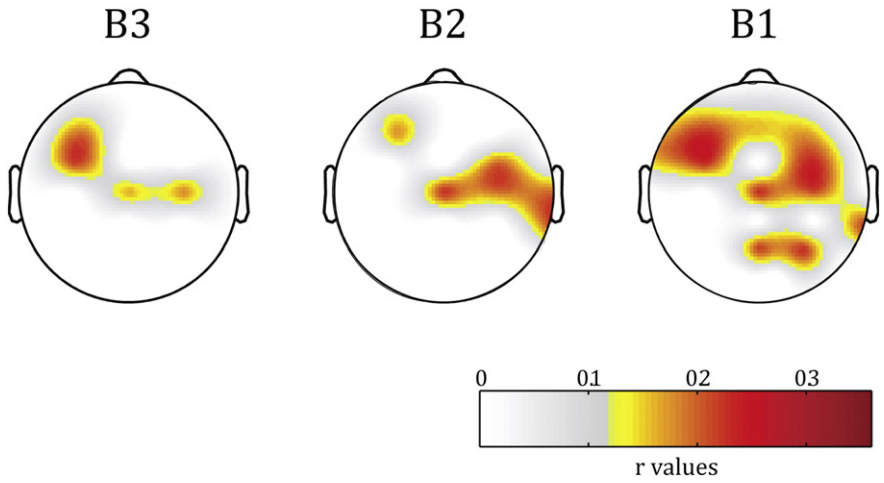


**Fig. 5.** Event-by-event variability of SSO amplitude parallels event-by-event variability of sigma expression. Each map plots the r-values of correlation coefficients between SSO amplitude and sigma expression calculated for each electrode. The three maps correspond to the three baseline windows B3, B2, B1. Figure shows that SSO amplitude of each event is predicted by baseline sigma activity in the fronto-central areas.

In conclusion, the present study demonstrates the importance of ongoing cortical activity in the generation and propagation of the SSO. In particular, sigma activity, which mostly represents the cortical expression of the thalamo-cortical *entrainment* in sleeping brains, sculpts structure, mapping and dynamics of full-fledged SSOs. Herein we have demonstrated these relationships in the first sleep cycle when the slow oscillations have their maximal expression due to the homeostatic pressure related to previous wakefulness activities (Riedner et al., 2007). On the contrary, spindle density exhibits a minimum in the first cycle and shows a linear increase across consecutive NREM episodes suggesting an inverse relation with the time course of SSOs (De Gennaro et al., 2000). According with the present results of sigma activity as a precursor of SSOs, we can hypothesize that sigma activity could be even more necessary for sustaining the proneness to bistability with the fading of the wake-related homeostatic pressure occurring after the first sleep cycle: We will investigate this putative relation with future long-term recordings.

We believe that understanding the role of alternating bistable events such as the SSOs and stable thalamo-cortical entrainment can shed light on the adaptive properties of the sleeping brain and provide insight into the pathomechanisms of sleep disturbances.

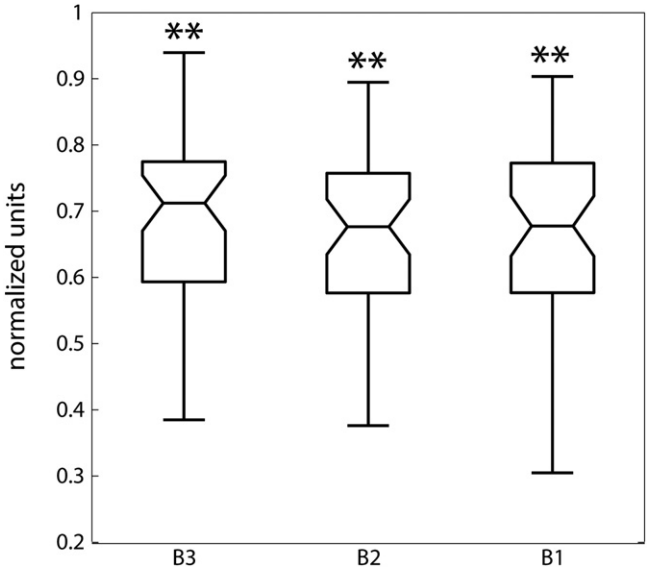


**Fig. 6.** SSO spreading is influenced by the amount of baseline sigma activity. The box plot shows the differences between baseline (B1, B2 and B3) sigma power estimated over each event spreading and that estimated at the same time over the related homologous electrodes, which are spared by the SSO travel. Differences are averaged over SSO events. Box plot description: the central mark is the median, the edges of the box are the 25th and 75th percentiles, the whiskers extend to the most extreme data points not considered outliers; ** $p < 0.01$, FDR corrected.

## Acknowledgments

The work was partially granted by the University of Pisa and by the ECSPLAIN-FP7-IDEAS-ERC-ref.338866.

## References

Allegrini, P., Paradisi, P., Menicucci, D., Laurino, M., Bedini, R., Piarulli, A., Gemignani, A., 2013. Sleep unconsciousness and breakdown of serial critical intermittency: new vistas on the global workspace. Chaos, Solitons Fractals 55, 32–43.

Amzica, F., Steriade, M., 1998. Electrophysiological correlates of sleep delta waves. Electroencephalogr. Clin. Neurophysiol. 107, 69–83.

Anaclet, C., Ferrari, L., Arrigoni, E., Bass, C.E., Saper, C.B., Lu, J., Fuller, P.M., 2014. The GABAergic parafacial zone is a medullary slow wave sleep-promoting center. Nat. Neurosci. 17, 1217–1224.

Ayoub, A., Aumann, D., Hörschelmann, A., Kouchekmanesch, A., Paul, P., Born, J., Marshall, L., 2013. Differential effects on fast and slow spindle activity, and the sleep slow oscillation in humans with carbamazepine and flunarizine to antagonize voltage-dependent Na + and Ca2+ channel activity. Sleep 36, 905–911.

Benjamini, Y., Yekutieli, D., 2001. The control of false discovery rate in multiple testing under dependency. Ann. Stat. 29 (4), 1165–1188.

Bonjean, M., Baker, T., Lemieux, M., Timofeev, I., Sejnowski, T., Bazhenov, M., 2011. Corticothalamic feedback controls sleep spindle duration in vivo. J. Neurosci. 31, 9124–9134.

Bonjean, M., Baker, T., Bazhenov, M., Cash, S., Halgren, E., Sejnowski, T., 2012. Interactions between core and matrix thalamocortical projections in human sleep spindle synchronization. J. Neurosci. 32 (15), 5250–5263.

Carrier, J., Land, S., Buysse, D.J., Kupfer, D.J., Monk, T.H., 2001. The effects of age and gender on sleep EEG power spectral density in the middle years of life (ages 20–60 years old). Psychophysiology 38, 232–242.

Chauvette, S., Volgushev, M., Timofeev, I., 2010. Origin of active states in local neocortical networks during slow sleep oscillation. Cereb. Cortex 20, 2660–2674.

Compte, A., Sanchez-Vives, M.V., McCormick, D.A., Wang, X.J., 2003. Cellular and network mechanisms of slow oscillatory activity (<1 Hz) and wave propagations in a cortical network model. J. Neurophysiol. 89, 2707–2725.

Contreras, D., Steriade, M., 1996. Spindle oscillation in cats: the role of corticothalamic feedback in a thalamically generated rhythm. J. Physiol. 490, 159–179.

Contreras, D., Timofeev, I., Steriade, M., 1996a. Mechanisms of long-lasting hyperpolarizations underlying slow sleep oscillations in cat corticothalamic networks. J. Physiol. 494, 251–264.

Contreras, D., Destexhe, A., Sejnowski, T.J., Steriade, M., 1996b. Control of spatiotemporal coherence of a thalamic oscillation by corticothalamic feedback. Science 274, 771–774.

Contreras, D., Destexhe, A., Sejnowski, T.J., Steriade, M., 1997. Spatiotemporal patterns of spindle oscillations in cortex and thalamus. J. Neurosci. 17, 1179–1196.

Crunelli, V., Hughes, S.W., 2010. The slow (<1 Hz) rhythm of non-REM sleep: a dialogue between three cardinal oscillators. Nat. Neurosci. 13 (1), 9–17.
Crunelli, V., David, F., Lőrincz, M.L., Hughes, S.W., 2015. The thalamocortical network as a single slow wave—generating unit. Curr. Opin. Neurobiol. 31, 72–80.
David, F., Schmiedt, J.T., Taylor, H.L., Orban, G., Di Giovanni, G., Uebele, V.N., Renger, J.J., Lambert, R.C., Leresche, N., Crunelli, V., 2013. Essential thalamic contribution to slow waves of natural sleep. J. Neurosci. 33 (50), 19599–19610.
De Gennaro, L., Ferrara, M., 2003. Sleep spindles: an overview. Sleep Med. Rev. 7 (5), 423–440.
De Gennaro, L., Ferrara, M., Bertini, M., 2000. Topographical distribution of spindles: variations between and within NREM sleep cycles. Sleep Res. Online 3, 155–160.
Dehghani, N., Cash, S.S., Chen, C.C., Hagler, D.J., Huang, M., Dale, A.M., Halgren, E., 2010. Divergent cortical generators of MEG and EEG during human sleep spindles suggested by distributed source modeling. PLoS One 5 (7), e11454.
Doran, S., 2003. The dynamic topography of individual sleep spindles. Sleep Res. Online 5, 133–139.
Esser, S.K., Hill, S.L., Tononi, G., 2007. Sleep homeostasis and cortical synchronization: I. Modeling the effects of synaptic strength on sleep slow waves. Sleep 30 (12), 1617–1630.
Feinberg, I., Campbell, I.G., 2010. Cerebral metabolism and sleep homeostasis: a comment on Vyazovskiy et al. Brain Res. Bull. 81 (1), 1–2.
Ferri, R., Bruni, O., Miano, S., Plazzi, G., Spruyt, K., Gozal, D., Terzano, M.G., 2006. The time structure of the cyclic alternating pattern during sleep. Sleep 29, 693–699.
Frohlich, F., Bazhenov, M., Timofeev, I., Steriade, M., Sejnowski, T.J., 2006. Slow state transitions of sustained neural oscillations by activity-dependent modulation of intrinsic excitability. J. Neurosci. 26 (23), 6153–6162.
Fuentealba, P., Steriade, M., 2005. The reticular nucleus revisited: intrinsic and network properties of a thalamic pacemaker. Prog. Neurobiol. 75 (2), 125–141.
Gemignani, A., Laurino, M., Provini, F., Piarulli, A., Barletta, G., d'Ascanio, P., Bedini, R., Lodi, R., Manners, D.N., Allegrini, P., Menicucci, D., Cortelli, P., 2012. Thalamic contribution to Sleep Slow Oscillation features in humans: a single case cross sectional EEG study in Fatal Familial Insomnia. Sleep Med. 13 (7), 946–952.
Halász, P., Terzano, M., Parrino, L., Bódizs, R., 2004. The nature of arousal in sleep. J. Sleep Res. 13, 1–23.
Hill, S., Tononi, G., 2005. Modeling sleep and wakefulness in the thalamocortical system. J. Neurophysiol. 93 (3), 1671–1698.
Hirata, A., Castro-Alamancos, M.A., 2010. Neocortex network activation and deactivation states controlled by the thalamus. 103 (3), 1147–1157.
Hughes, S.W., Crunelli, V., 2005. Thalamic mechanisms of EEG alpha rhythms and their pathological implications. Neuroscientist 11 (4), 357–372.
Hughes, S.W., Crunelli, V., 2007. Just a phase they're going through: the complex interaction of intrinsic high-threshold bursting and gap junctions in the generation of thalamic alpha and theta rhythms. Int. J. Psychophysiol. 64, 3–17.
Hughes, S.W., Lorincz, M.L., Parri, H.R., Crunelli, V., 2011. Infraslow (<0.1 Hz) oscillations in thalamic relay nuclei basic mechanisms and significance to health and disease states. Prog. Brain Res. 193, 145–162.
Iber, C., Ancoli-Israel, S., Chesson, A., Quan, S.F., 2007. The AASM Manual for the Scoring of Sleep and Associated Events: Rules, Terminology and Technical Specifications. American Academy of Sleep Medicine, Westchester, IL.
James, C.J., Gibson, O.J., 2003. Temporally constrained ICA: an application to artifact rejection in electromagnetic brain signal analysis. IEEE Trans. Biomed. Eng. 50, 1108–1116.
Klimesch, W., 1999. EEG alpha and theta oscillations reflect cognitive and memory performance: a review and analysis. Brain Res. Rev. 29, 169–195.
Laurino, M., Menicucci, D., Piarulli, A., Mastorci, F., Bedini, R., Allegrini, P., Gemignani, A., 2014. Disentangling different functional roles of evoked K-complex components: mapping the sleeping brain while quenching sensory processing. NeuroImage 86, 433–445.
Marini, G., Gritti, I., Mancia, M., 1989. Changes in EEG spindle activity induced by ibotenic acid lesions of medialis dorsalis thalamic nuclei in the cat. Brain Res. 500, 395–399.
Massimini, M., Huber, R., Ferrarelli, F., Hill, S., Tononi, G., 2004. The sleep slow oscillation as a traveling wave. J. Neurosci. 24, 6862–6870.
Menicucci, D., Piarulli, A., Debarnot, U., d'Ascanio, P., Landi, A., Gemignani, A., 2009. Functional structure of spontaneous sleep slow oscillation activity in humans. PLoS One 4, e7601.
Menicucci, D., Piarulli, A., Allegrini, P., Laurino, M., Mastorci, F., Sebastiani, L., Bedini, R., Gemignani, A., 2013. Fragments of wake-like activity frame down-states of sleep slow oscillations in humans: new vistas for studying homeostatic processes during sleep. Int. J. Psychophysiol. 89, 151–157.
Mölle, M., Marshall, L., Gais, S., Born, J., 2002. Grouping of spindle activity during slow oscillations in human non-rapid eye movement sleep. J. Neurosci. 22, 10941–10947.
Montagna, P., Provini, F., Plazzi, G., Vetrugno, R., Gallassi, R., Pierangeli, G., Ragno, M., Cortelli, P., Perani, D., 2002. Bilateral paramedian thalamic syndrome: abnormal circadian wake–sleep and autonomic functions. J. Neurol. Neurosurg. Psychiatry 73, 772–774.
Montagna, P., Gambetti, P., Cortelli, P., Lugaresi, E., 2003. Familial and sporadic fatal insomnia. Lancet Neurol. 2, 167–176.
Parrino, L., Halasz, P., Tassinari, C.A., Terzano, M.G., 2006. CAP, epilepsy and motor events during sleep: the unifying role of arousal. Sleep Med. Rev. 10, 267–285.
Piantoni, G., Poil, S., Linkenkaer-Hansen, K., Verweij, I.M., Ramautar, J.R., Van Someren, E.J.W., Van Der Werf, Y.D., 2013a. Individual differences in white matter diffusion affect sleep oscillations. J. Neurosci. 33, 227–233.
Piantoni, G., Astill, R.G., Raymann, R.J.E.M., Vis, J.C., Coppens, J.E., Van Someren, E.J.W., 2013b. Modulation of gamma and spindle-range power by slow oscillations in scalp sleep EEG of children. Int. J. Psychophysiol. 89, 252–258.
Piarulli, A., Menicucci, D., Gemignani, A., Olcese, U., d'Ascanio, P., Pingitore, A., Bedini, R., Landi, A., 2010. Likeness-based detection of sleep slow oscillations in normal and altered sleep conditions: application on low-density EEG recordings. IEEE Trans. Biomed. Eng. 57, 363–372.
Riedner, B.A., Vyazovskiy, V.V., Huber, R., Massimini, M., Esser, S.K., Murphy, M., Tononi, G., 2007. Sleep homeostasis and cortical synchronization: III. A high-density EEG study of sleep slow waves in humans. Sleep 30, 1643–1657.
Rigas, P., Castro-Alamancos, M.A., 2007. Thalamocortical Up states: differential effects of intrinsic and extrinsic cortical inputs on persistent activity. J. Neurosci. 27 (16), 4261–4272.
Sanchez-Vives, M.V., Mattia, M., Compte, A., Perez-Zabalza, M., Winograd, M., Descalzo, V.F., Reig, R., 2010. Inhibitory modulation of cortical up states. J. Neurophysiol. 104, 1314–1324.
Santamaria, J., Pujol, M., Orteu, N., Solanas, A., Cardenal, C., Santacruz, P., Chimeno, E., Moon, P., 2000. Unilateral thalamic stroke does not decrease ipsilateral sleep spindles. Sleep 23, 333–339.
Sejnowski, T.J., Destexhe, A., 2000. Why do we sleep? Brain Res. 886, 208–223.
Shu, Y., Hasenstaub, A., McCormick, D.A., 2003. Turning on and off recurrent balanced cortical activity. Nature 423, 288–293.
Steriade, M., 2000. Corticothalamic resonance, states of vigilance and mentation. Neuroscience 101, 243–276.
Steriade, M., 2004. Acetylcholine systems and rhythmic activities during the waking-sleep cycle. Prog. Brain Res. 145, 179–196.
Steriade, M., 2006. Grouping of brain rhythms in corticothalamic systems. Neuroscience 137, 1087–1106.
Steriade, M., Deschenes, M., 1984. The thalamus as a neuronal oscillator. Brain Res. 320, 1–63.
Steriade, M., Nuñez, A., Amzica, F., 1993a. A novel slow (<1 Hz) oscillation of neocortical neurons in vivo: depolarizing and hyperpolarizing components. J. Neurosci. 13, 3252–3265.
Steriade, M., Contreras, D., Curró Dossi, R., Nuñez, A., 1993b. The slow (<1 Hz) oscillation in reticular thalamic and thalamocortical neurons: scenario of sleep rhythm generation in interacting thalamic and neocortical networks. J. Neurosci. 13, 3284–3299.
Steriade, M., Amzica, F., Nunez, A., 1993c. Cholinergic and noradrenergic modulation of the slow (approximately 0.3 Hz) oscillation in neocortical cells. J. Neurophysiol. 70 (4), 1385–1400.
Terzano, M.G., Parrino, L., 1993. Clinical applications of cyclic alternating pattern. Physiol. Behav. 54, 807–813.
Timofeev, I., Chauvette, S., 2011. Thalamocortical oscillations: local control of EEG slow waves. Curr. Top. Med. Chem. 11, 2457–2471.
Timofeev, I., Chauvette, S., 2013. The spindles: are they still thalamic? Sleep 36, 825.
Timofeev, I., Grenier, F., Bazhenov, M., Sejnowski, T.J., Steriade, M., 2000. Origin of slow cortical oscillations in deafferented cortical slabs. Cereb. Cortex 10 (12), 1185–1199.
Tononi, G., Cirelli, C., 2014. Sleep and the price of plasticity: from synaptic and cellular homeostasis to memory consolidation and integration. Neuron 81 (1), 12–34.
Valencia, M., Artieda, J., Bolam, J.P., Mena—Segovia, J., 2013. Dynamic interaction of spindles and gamma activity during cortical slow oscillations and its modulation by subcortical afferents. PLoS ONE 8 (7) e67540.
Vanhatalo, S., Palva, J.M., Holmes, M.D., Miller, J.W., Voipio, J., Kaila, K., 2004. Infraslow oscillations modulate excitability and interictal epileptic activity in the human cortex during sleep. Proc. Natl. Acad. Sci. U. S. A. 101, 5053–5057.
Vanhatalo, S., Voipio, J., Kaila, K., 2005. Full-band EEG (FbEEG): an emerging standard in electroencephalography. Clin. Neurophysiol. 116, 1–8.
Vijayan, S., Kopell, N.J., 2012. Thalamic model of awake alpha oscillations and implications for stimulus processing. Proc. Natl. Acad. Sci. U. S. A. 109 (45), 18553–18558.
Vyazovskiy, V.V., Riedner, B.A., Cirelli, C., Tononi, G., 2007. Sleep homeostasis and cortical synchronization: II. A local field potential study of sleep slow waves in the rat. Sleep 30 (12), 1631–1642.
Vyazovskiy, V.V., Olcese, U., Lazimy, Y.M., Faraguna, U., Esser, S.K., Williams, J.C., Cirelli, C., Tononi, G., 2009. Cortical firing and sleep homeostasis. Neuron 63, 865–878.
Ward, L.M., 2011. The thalamic dynamic core theory of conscious experience. Conscious. Cogn. 20 (2), 464–486.
Wester, J.C., Contreras, D., 2013. Generating waves in corticothalamocortical networks. Neuron 77 (6), 995–997.
Wilson, M.T., Steyn-Ross, D.A., Sleigh, J.W., Steyn-Ross, M.L., Wilcocks, L.C., Gillies, I.P., 2006. The K-complex and slow oscillation in terms of a mean-field cortical model. J. Comput. Neurosci. 21, 243–257.